Global Biogeochemical Cycles

RESEARCH ARTICLE
10.1029/2024GB008358

Biological Responses to Ocean Acidification Are Changing the Global Ocean Carbon Cycle

R. C. Barrett[1], B. R. Carter[2,3], A. J. Fassbender[2], B. Tilbrook[4,5], R. J. Woosley[6], K. Azetsu-Scott[7], R. A. Feely[2], C. Goyet[8], M. Ishii[9], A. Murata[10], and F. F. Pérez[11]

[1]School of Oceanography, University of Washington, Seattle, WA, USA, [2]Pacific Marine Environmental Laboratory, Seattle, WA, USA, [3]Cooperative Institute for Climate, Ocean, and Ecosystem Studies, University of Washington, Seattle, WA, USA, [4]Environment Research Unit, Commonwealth Scientific and Research Organisation (CSIRO), Hobart, TAS, Australia, [5]Australian Antarctic Program Partnership, University of Tasmania, Hobart, TAS, Australia, [6]Department of Earth, Atmospheric, and Planetary Sciences, Center for Sustainability Science and Policy, Massachusetts Institute for Technology, Cambridge, MA, USA, [7]Department of Fisheries and Oceans, Bedford Institute of Oceanography, Dartmouth, NS, Canada, [8]Espace-Dev UMR 228, Université de Perpignan Via Domitia, IRD, UM, UA, UG, Perpignan, France, [9]Climate and Geochemistry Research Department, Meteorological Research Institute, Japan Meteorological Agency, Tsukuba, Japan, [10]Research Institute for Global Change, Japan Agency for Marine-Earth Science and Technology (JAMSTEC), Yokosuka, Japan, [11]Instituto de Investigaciones Marinas (IIM), CSIC, Vigo, Spain

Abstract Increased oceanic uptake of CO_2 due to rising anthropogenic emissions has caused lowered pH levels (ocean acidification) that are hypothesized to diminish biotic calcification and reduce the export of total alkalinity (A_T) as carbonate minerals from the surface ocean or their burial in coastal sediments. This "CO_2-biotic calcification feedback" is a negative feedback on atmospheric CO_2, as elevated levels of surface A_T increase the ocean's capacity to uptake CO_2. We detect signatures of this feedback in the global ocean for the first time using repeat hydrographic measurements and seawater property prediction algorithms. Over the course of the past 30 years, we find an increase in global surface A_T of 0.072 ± 0.023 μmol kg^{-1} yr^{-1}, which would have caused approximately 20 Tmol of additional A_T to accumulate in the surface ocean. This finding suggests that anthropogenic CO_2 emissions are measurably perturbing the cycling of carbon on a planetary scale by disrupting biological patterns. More observations of A_T would be required to understand the effects of this feedback on a regional basis and to fully characterize its potential to reduce the efficiency of marine carbon dioxide removal technology.

Plain Language Summary Human activities are causing more carbon dioxide (CO_2) to be absorbed by the oceans from the atmosphere, leading to decreasing ocean pH levels (ocean acidification). Acidification slows down biotic calcification, the process by which many marine organisms build their shells and skeletons. Lowered biotic calcification is hypothesized to reduce the carbon moving from the ocean's surface to the deep when these organisms die and sink. This decrease in the amount of sinking shells leads to a buildup in total alkalinity (A_T) in surface waters, which helps the ocean absorb more CO_2—a natural feedback mechanism that could limit the rise of atmospheric CO_2. We have identified signs of this feedback in the global ocean. Our findings show that the A_T in the ocean's surface is increasing by 0.072 ± 0.023 μmol per kilogram per year, which would have caused the amount of human-emitted carbon in the ocean to increase by about 0.20 PgC since the 1990s. This shows that the chemistry of the oceans is changing as human-produced CO_2 emissions cause shifts in the patterns of life and death of some marine organisms. More data on A_T is needed to better quantify this feedback and its impacts.

Key Points:

- We find evidence of a long-term trend in alkalinity in the surface ocean using measurements and seawater property prediction algorithms
- We determine this trend is likely driven by the CO_2-biotic calcification feedback, a hypothesized negative feedback on atmospheric CO_2
- Ocean chemistry is changing globally due to shifting patterns in the ecology of calcifying organisms caused by anthropogenic CO_2 emissions

Supporting Information:

Supporting Information may be found in the online version of this article.

Correspondence to:

R. C. Barrett,
rcbarr1@uw.edu

Citation:

Barrett, R. C., Carter, B. R., Fassbender, A. J., Tilbrook, B., Woosley, R. J., Azetsu-Scott, K., et al. (2025). Biological responses to ocean acidification are changing the global ocean carbon cycle. *Global Biogeochemical Cycles*, *39*, e2024GB008358. https://doi.org/10.1029/2024GB008358

Received 13 SEP 2024
Accepted 24 FEB 2025
Corrected 18 APR 2025

This article was corrected on 18 APR 2025. See the end of the full text for details.

Author Contributions:

Conceptualization: R. C. Barrett, B. R. Carter, A. J. Fassbender, B. Tilbrook, R. J. Woosley
Data curation: R. C. Barrett
Formal analysis: R. C. Barrett, B. R. Carter
Funding acquisition: B. R. Carter
Investigation: R. C. Barrett
Methodology: R. C. Barrett, B. R. Carter
Project administration: R. C. Barrett, B. R. Carter
Resources: B. R. Carter

1. Introduction

From the 1960s to the present day, the Earth's oceans have absorbed about 25% of anthropogenic carbon dioxide (CO_2) emissions, reducing atmospheric CO_2 concentrations and slowing the rate of climate change (Friedlingstein et al., 2023; Gruber et al., 2023). The resulting increased levels of CO_2 in the ocean have caused a global pH reduction in seawater, termed ocean acidification, which has begun to alter marine ecosystems and put the human communities that rely on them at risk (Doney et al., 2009, 2020; Gattuso et al., 2015). Biotic calcification by organisms such as coccolithophores, pteropods, foraminifera, and corals remove carbon from the surface ocean in the form of calcium carbonate ($CaCO_3$) and other carbonate minerals and export it to the deep ocean (Berelson et al., 2007; Boudreau et al., 1999, 2018; Subhas et al., 2022; Milliman, 1993; Milliman et al., 1999). However, it

Software: R. C. Barrett, B. R. Carter
Supervision: B. R. Carter
Validation: R. C. Barrett
Visualization: R. C. Barrett
Writing – original draft: R. C. Barrett, B. R. Carter
Writing – review & editing: R. C. Barrett, B. R. Carter, A. J. Fassbender, B. Tilbrook, R. J. Woosley, K. Azetsu-Scott, R. A. Feely, C. Goyet, M. Ishii, A. Murata, F. F. Pérez

has been hypothesized that ocean acidification could reduce this "$CaCO_3$ pump" by damaging calcifying organisms, disfavoring $CaCO_3$ production, and speeding $CaCO_3$ dissolution (Heinze, 2004; Ilyina et al., 2009; Zondervan et al., 2001).

Total alkalinity (A_T), or the excess of hydrogen ion acceptors over hydrogen ion donors in seawater, is a parameter that describes the carbonate system of seawater and does not change with air-sea CO_2 exchange (Dickson, 1981). However, the concentration of A_T does shift with changes in biotic calcification and carbonate mineral export. If carbonate mineral export rates are decreasing, less A_T is transported to the depth, which would cause a relative buildup of A_T in the surface ocean. Trends in A_T, therefore, can be used to assess whether patterns in biotic calcification and export are changing over time.

Theoretically, an increase in surface A_T due to lowered calcification rates would enhance the ocean's buffering capacity and increase the drawdown of CO_2, dampening atmospheric CO_2 rise. This "CO_2-biotic calcification feedback" would cause greater uptake of CO_2 into surface waters and the ocean interior (Ridgwell et al., 2007; Zondervan et al., 2001). However, the magnitude of the response is uncertain and would vary regionally based on the background buffering capacity. Models show that the CO_2-biotic calcification feedback may even play a larger role in regulating ocean CO_2 content than the well-established CO_2-ocean warming feedback, where increased seawater temperatures reduce the amount of inorganic carbon in the ocean present at air-sea CO_2 equilibrium (Zhang & Cao, 2016). Furthermore, Earth System Model outputs show differences in both magnitude and sign of the trend in surface alkalinity over time, meaning that existing parameterizations may not adequately represent this feedback (Jiang et al., 2023).

In this work, repeat hydrographic sections of total alkalinity measurements (A_T) are used in conjunction with seawater property prediction algorithms to detect trends in A_T consistent with the CO_2-biotic calcification feedback in observational data sets. This phenomenon is hypothesized to have emerged, or become statistically significant above natural variability, only in this decade (Schlunegger et al., 2019). In this study, we observe a long-term (>30 years) trend in surface ocean A_T, which we find can likely be attributed to a global negative feedback in biotic calcification or carbonate mineral export. This indicates that anthropogenic CO_2 emissions are changing the marine carbon cycle's controls on Earth's climate through biological mechanisms.

2. Data and Methods

2.1. Data Used: GLODAPv2.2023

Data made available by the Global Ocean Data Analysis Project (GLODAP) version 2.2023 were used for this analysis (Lauvset et al., 2022, 2023; Olsen et al., 2019, 2020). GLODAP provides a collection of ship-based ocean biogeochemical data, including marine carbonate system data, that has undergone secondary quality control to improve data product consistency. Cruise records from the current version GLODAPv2.2023 were filtered to include only data from cruises on transects occupied by the Global Ocean Ship-Based Hydrographic Investigations Program (GO-SHIP). All data used in this analysis were collected from cruises associated with GO-SHIP, the World Ocean Circulation Experiment (WOCE)/the Joint Global Ocean Flux Study (JGOFS), Climate and Ocean: Variability, Predictability, and Change (CLIVAR), and Southern Ocean Carbon and Climate Observations and Modeling (SOCCOM).

Data were further filtered to ensure only the highest quality observations were included in this analysis. Only A_T data that were flagged by GLODAP as "2," meaning "acceptable," were kept. Additionally, any A_T data that were marked by GLODAP as "calculated" instead of "measured" were excluded. To constrain the analysis to only the open ocean, points with associated salinity measurements that fell outside 30–37 (i.e., estuaries) were excluded. Cruises were trimmed to keep only the data points that were located on GO-SHIP transects, typically omitting only "test cast" stations. Following the filtering and trimming processes, 230,572 A_T measurements spread across 201 total cruises were available for analysis, which were collected between 1 September 1991 and 4 October 2021. Figure 1 shows the spatial coverage of data.

The seawater A_T measurements used in this study have been collected by the global oceanographic community following standard operating procedures (Dickson et al., 2007). These measurements have benefitted from the regular use of a community reference material since the early 1990s (Dickson et al., 2003). The exact titration methods vary between research groups (Carter, Sharp, Dickson, et al., 2024), and there is some indication that different methods can return different values for identical seawater when organic or unidentified contributions to

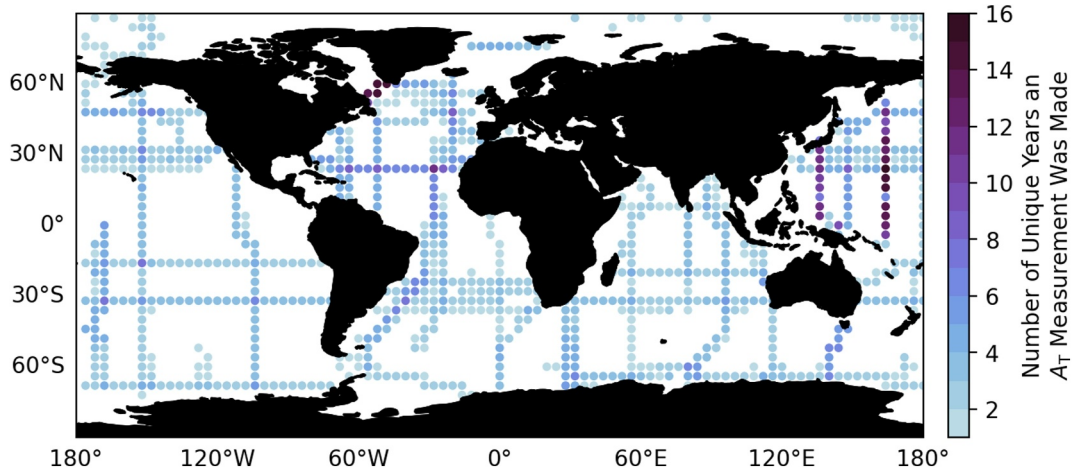

Figure 1. Map of locations of A_T measurements (rounded to the nearest 4° of latitude and longitude) available from GLODAPv2.2023 that were used in this analysis following all quality control steps. Coloring shows the number of unique years where measurements are available at each location.

A_T with a pK_a close to approximately four are present (Sharp & Byrne, 2020). The GLODAPv2 adjustments may have accounted for these variations to an unknown degree (Olsen et al., 2019). Inter-laboratory calibration studies show variations between measurements across laboratories (Bockmon & Dickson, 2015). The random variability in a subset of open-ocean repeat hydrographic A_T measurements (which includes cruise-to-cruise variations) has recently been estimated as (1σ) 2 μmol kg^{-1} before the GLODAPv2 adjustment procedure (Carter, Sharp, García-Ibáñez, et al., 2024). This is smaller than the uncertainty across all A_T measurements, which is estimated to be 2.4 μmol kg^{-1} (Carter, Sharp, García-Ibáñez, et al., 2024). We repeat this analysis here and estimate an uncertainty in A_T of 2 μmol kg^{-1} for the subset of cruises involved in the present study (Figure 1). However, we caution that this analysis further limits the cruises considered to the subset of the cruises we use that have overdetermined carbonate chemistry measurements.

2.2. Algorithms Used: Empirical Seawater Property Estimation Routines (ESPERs)

Empirical Seawater Property Estimation Routines (ESPERs) are algorithms trained on GLODAPv2.2020 data that are able to predict seawater properties, including A_T, at a given location. Salinity, with which A_T has the strongest covariance, and optional additional seawater property information are used to make each prediction (Carter et al., 2021). Two independent algorithms are available–ESPER_LIR, which is based on locally interpolated regressions, and ESPER_NN, which uses a neural network approach.

In this study, we quantify the correlation between time and the evolving difference between A_T measurements and co-located ESPER A_T estimates. ESPERs do not include a long-term temporal component in the prediction of A_T, which makes it possible for ESPER-generated predictions to serve as a counterfactual that represents conditions in the ocean under a steady-state scenario. The difference between a measured property of seawater and the ESPER estimate of the same property (henceforth defined for A_T as ΔA_T) allows for the presence and magnitude of any long-term climatic changes in seawater to be assessed. It should be noted that a temporal component in these estimates may be implicit due to long-term trends in the predictors used to produce the estimates (Figure S1 in Supporting Information S1), which would contribute to uncertainty in ESPER predictions. We explore this possibility further when alternative hypotheses are presented (see Section 4). Furthermore, the sign of the trend in A_T over time may be different from the sign of ΔA_T over time, as A_T is the absolute measurement of total alkalinity, while ΔA_T represents the difference between the measured and ESPER-predicted A_T value.

This same approach to determining trends in a variable of interest in the marine carbonate system was used in fitting a term in the development of the Locally Interpolated pH Regression (LIPHR) algorithm to account for the temporal effect of ocean acidification on pH predictions (Carter et al., 2018). The method found a global surface ocean acidification rate of −0.0018 ± 0.0003 pH units per year, which compares very closely with independent estimates for a similar time period of −0.0017 ± 0.001 pH units per year (Ma et al., 2023).

Table 1
Combinations of Input Parameters Used to Calculate A_T in Each ESPER Equation

Equation	Input properties
1	S_P, T, NO_3^-, O_2, SiO_4^{4-}
2	S_P, T, NO_3^-, SiO_4^{4-}
3	S_P, T, O_2, SiO_4^{4-}
4	S_P, T, SiO_4^{4-}
5	S_P, T, NO_3^-, O_2
6	S_P, T, NO_3^-
7	S_P, T, O_2
8	S_P, T
9	S_P, NO_3^-, O_2, SiO_4^{4-}
10	S_P, NO_3^-, SiO_4^{4-}
11	S_P, O_2, SiO_4^{4-}
12	S_P, SiO_4^{4-}
13	S_P, NO_3^-, O_2
14	S_P, NO_3^-
15	S_P, O_2
16	S_P

Note. "S_P" represents salinity on the practical scale, "T" represents temperature (°C), "NO_3^-" represents nitrate (μmol kg^{-1}), "O_2" represents dissolved oxygen (μmol kg^{-1}), and "SiO_4" represents silicate (μmol kg^{-1}).

Both ESPER routines (ESPER_LIR and ESPER_NN) were used to predict A_T at the location and time of each A_T measurement used in this study. There are 16 equations that can be used in each ESPER for seawater property predictions, each of which requires a different combination of input seawater property measurements. For A_T, this is outlined below in Table 1. A_T varies most strongly with salinity, but is also correlated with changes in temperature, oxygen, and macronutrient distributions. Salinity is a required input in all 16 equations and the other predictors are each used in half of the 16 equations.

The unweighted ensemble mean of the estimates produced by the 16 equations was used to calculate ΔA_T for each ESPER routine. Plancherel et al. (2013) showed that errors using multiple linear regression (MLR) algorithms tend to be uncorrelated from each other, and therefore benefit somewhat from ensemble mean averaging. While some of the 16 equations we use in our ensemble average produce estimates with higher fidelity than others, Carter et al. (2019) found the benefit of weighting ensemble members by the inverse of their uncertainty to be limited when estimating anthropogenic carbon accumulation rates. For that study and this one, the important quantity is how the estimate varies over time rather than the value of the estimate, so we again average ensemble members without any prior weighting. The standard deviation of the trend in ΔA_T across the 16 equations is also calculated (u_{ESPER}) as an estimate of one component of uncertainty in the trend.

2.3. Statistical Analyses

Measurements from the surface ocean as well as the full depth of the water column were separately analyzed, as trends in alkalinity due to ocean acidification are expected to be visible first in the surface ocean (Carter et al., 2016). Multiple definitions of "surface ocean" were tested, including 10 m depth, 25 m depth, 100 m depth, average monthly mean mixed layer depth, and maximum monthly maximum mixed layer depth, and the depth selected had little effect on the results. Climatology described by Holte et al., 2017 were used for average monthly mean mixed layer depth and maximum monthly maximum mixed layer depth. For the following analysis, a surface ocean depth of 25 m will be used. "Full depth" indicates that all available depths of measurements were used, which includes all depths from the surface to a maximum of 6,742 m. The average depth of measurement was 1,426 m. 95% of measurements fell between 0 and 4,500 m in depth.

Two linear regression techniques were used to analyze changes in ΔA_T over time. Robust linear regression (RLM), using maximum likelihood type estimation (M-estimation) with Huber's t function, was performed to reduce the sensitivity of the regression results to outliers in A_T measurements (Figure S2 in Supporting Information S1). Robust regression is an established practice used to reduce the influence of outliers (Andersen, 2007). For comparison purposes–and to ensure our results were not overly sensitive to our robust regression weighting choices–ordinary least squares (OLS) regression was also performed. No temporal or spatial patterns in outliers were detected (Figure S3 in Supporting Information S1).

A Monte Carlo analysis was performed to account for uncertainty in GLODAP data by adding offsets to the data randomly selected from a Gaussian distribution centered at zero with a standard deviation of 2 μmol kg^{-1}, which represents the accepted uncertainty in open-ocean repeat hydrographic A_T measurements (see Section 2.1; Carter, Sharp, García-Ibáñez, et al., 2024). Two variations of the Monte Carlo analysis were conducted. In the first "per-cruise transect" method, a random offset was selected for each cruise to be applied to every A_T measurement taken on that cruise to represent systematic sampling errors that may have occurred. 1,000 repetitions of the Monte Carlo simulations were performed, and the standard deviation of the resulting trends in ΔA_T is taken to represent sampling uncertainty (u_{sample}). This uncertainty differs from the individual measurement uncertainty (2 μmol kg^{-1}) in that it does not represent uncertainty in a single measurement of A_T, but rather the uncertainty in the trend in ΔA_T over time possible when all individual measurements are taken together.

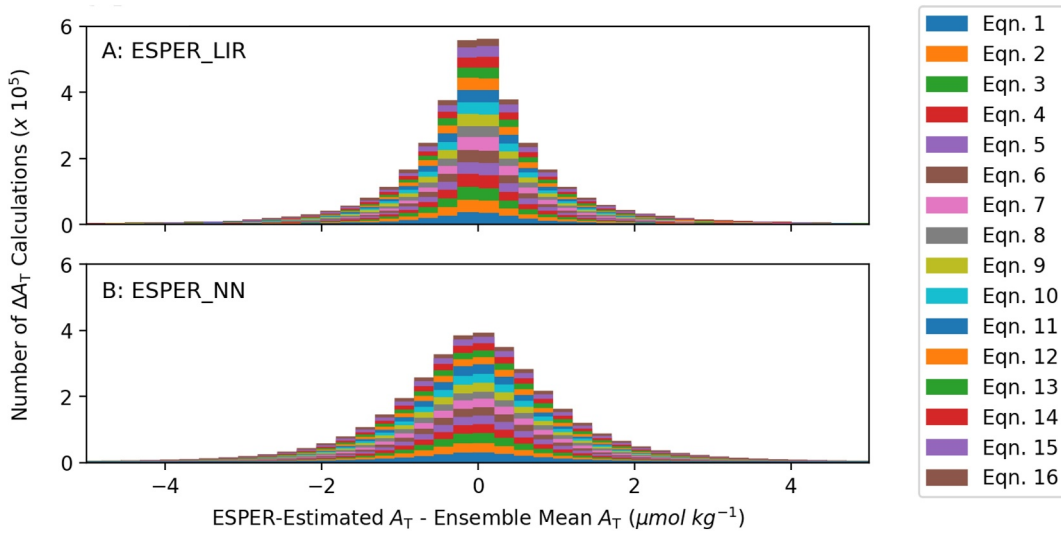

Figure 2. Difference between the ESPER-predicted A_T and ensemble mean for each ESPER equation. Each data point represented in the histogram is one ESPER prediction. Subplot A uses ESPER_LIR as the counterfactual; subplot B uses ESPER_NN.

Sampling uncertainty (u_{sample}) is summed in quadrature (the square root of the sum of squares) with u_{ESPER} (previously defined in Section 2.2) to estimate total uncertainty (U). Results were analyzed on both a global, regional, and per-cruise transect basis. The per-cruise transect analysis was performed only when two or more reoccupations existed in that transect. In the second "per-point" method, a unique random offset was applied to every measurement used in the analysis, but it was found that this style of Monte Carlo simulation had no meaningful impact on the trend in ΔA_T due to the large number of measurements (Figures S4 and S5 in Supporting Information S1).

A flow chart outlining the methodology utilized in this work is included as Figure S6 in Supporting Information S1.

3. Results

Across all equations, the average ΔA_T calculated using ESPER_LIR was −0.29 μmol kg^{-1}, with a standard deviation of 4.27 μmol kg^{-1}. The average ΔA_T using ESPER_NN was −0.26 μmol kg^{-1}, with a standard deviation of 4.23 μmol kg^{-1}. Mean ΔA_T was statistically indistinguishable across all 16 ESPER equations (Figure 2). Adding more predictors decreases the standard deviation in ΔA_T, consistent with a known improvement in the estimate fidelity in the GLODAPv2.2020 training product, which has strong overlap with the subset of GLODAPv2.2023 we use for this study (Carter et al., 2021). The number of viable ΔA_T values decreases by 6.3% as the number of predictors used increases from 1 to 5, because each ESPER calculation is only performed if all the required predictors were concurrently measured.

A statistically significant positive temporal trend in ΔA_T in the surface ocean (<25 m) was found using both ordinary least squares (OLS) regression and robust linear model (RLM) regression (Table 2, Figure 3). In other words, the measured A_T values are increasing compared to the ESPER-calculated counterfactual, which indicates that A_T levels have been increasing on a global scale in the surface ocean over the past three decades.

Trends in ΔA_T in the surface ocean are positive and greater than twice the overall uncertainty in the trends (i.e., >2σ, or >95% confidence). A positive trend is also seen across the full ocean depth, though this trend is only statistically significant when considering the uncertainty in the slope term fit by the linear regression alone. The deep trend is not statistically significant when considering the much larger overall uncertainty (U) estimate that accounts for the likely errors in measurements of A_T and ESPER estimates. Lessening the weight of outliers with RLM always results in a trend that is both more positive and significant, but the statements regarding significance remain unchanged for OLS.

Table 2
Trends in ΔA_T Over Time (μmol kg^{-1} yr^{-1}) for Each Region Calculated by Robust Linear Model (RLM) and Ordinary Least Squares (OLS) Regression With Associated Uncertainties

	RLM		OLS	
	ESPER_LIR	ESPER_NN	ESPER_LIR	ESPER_NN
Surface Ocean (<25 m)	0.072 ± 0.023	0.070 ± 0.023	0.054 ± 0.023	0.056 ± 0.023
Full Ocean Depth	0.011 ± 0.022	0.005 ± 0.022	0.008 ± 0.022	0.003 ± 0.022

Note. ESPER_LIR and ESPER_NN were each used as counterfactuals, and the trends in the surface ocean (<25 m) and for the full depth of measurements are shown for each regression type and counterfactual.

The majority of uncertainty U in each trend in ΔA_T is derived from u_{sample}, which is calculated using the Monte Carlo simulation (Figure 4). Monte Carlo analysis shows high confidence in a positive trend in surface ocean ΔA_T over time. On average across the set of 1,000 Monte Carlo runs, the standard deviation of the simulated trends in surface ΔA_T is 0.022 μmol kg^{-1} yr^{-1}. Even with this uncertainty, 99.3% of simulations result in a positive trend with ESPER_LIR as the counterfactual (99.5% with ESPER_NN). This does not hold for the full-ocean analysis, as much smaller trends in ΔA_T are found relative to estimated uncertainties (standard deviation of 0.022 μmol kg^{-1} yr^{-1}). A positive trend is only seen 65.5% of the time (with ESPER_LIR as counterfactual, 55.9% with ESPER_NN).

Uncertainty analysis shows that trends in ΔA_T over time along individual transects, which are sometimes apparent from regression statistics, are not able to be confidently distinguished from either the global trend or from the null hypothesis that changes are the result of measurement uncertainties (Figure S7 in Supporting Information S1). Most of the OLS-calculated trends in ΔA_T across 1,000 Monte Carlo runs do not show a clear positive or negative result (Figure S8 in Supporting Information S1). Furthermore, a visual analysis of the spatial distribution of

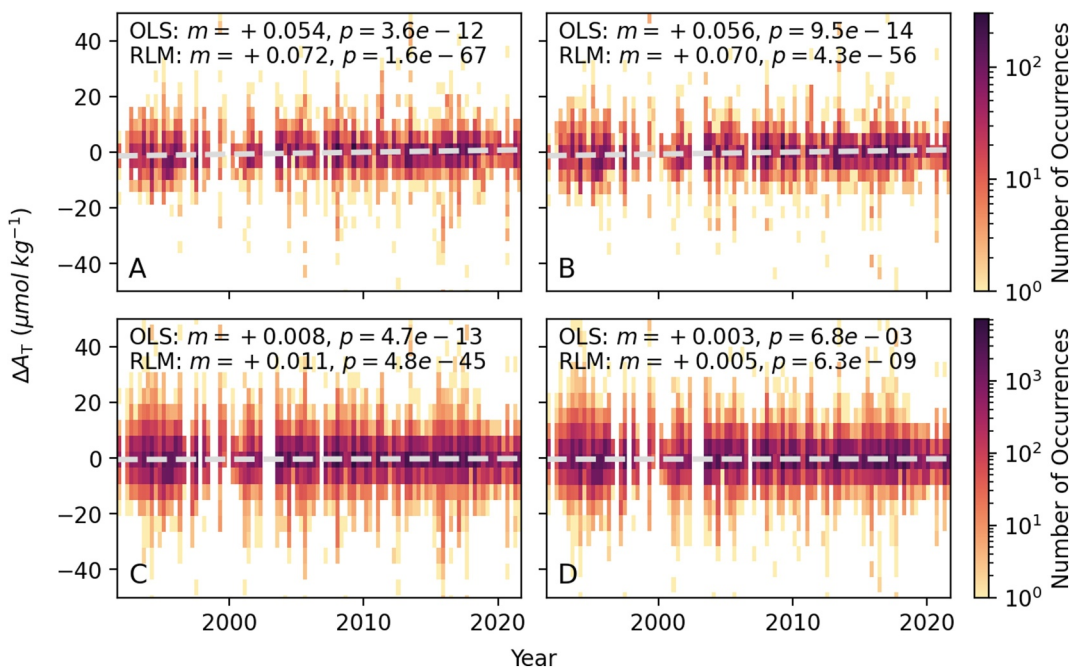

Figure 3. Ordinary least squares (OLS) and robust linear regression (RLM) calculated for surface values only (<25 m depth, subplots A,B) and over the full depth of available data (subplots C, D) using the ensemble mean of each ESPER routine (A, C: ESPER_LIR, B, D: ESPER_NN). RLM regression line is overlaid on a two-dimensional histogram showing the difference between the measured A_T and ESPER-estimated A_T (ΔA_T) over time. Slopes (m) and p-values (p) for both regression techniques are shown on each subplot. Positive slopes on all plots indicate that the measured A_T is becoming larger than the co-located ESPER-estimated A_T.

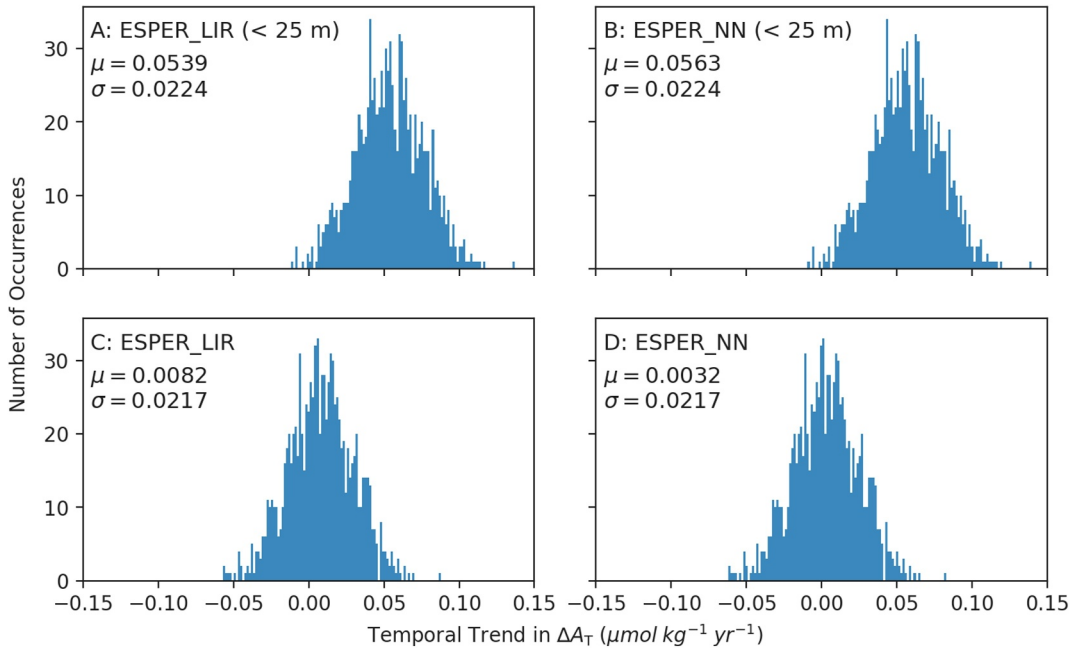

Figure 4. Monte Carlo simulation results. During each run of the Monte Carlo simulation, a single offset randomly chosen from a normal distribution centered at zero with standard deviation 2 μmol kg^{-1} was applied to all of the measurements made on a single cruise transect, such that all measurements on each cruise were offset by the same amount but each cruise was offset by a different random amount. Histogram shows the slope (μ) and standard deviation (σ) of the difference in measured A_T and ESPER-estimated A_T (ΔA_T) over time obtained by ordinary least squares regression for each of the 1,000 Monte Carlo simulation runs. Subplots A-B: surface values (<25 m depth); subplots C-D: full depth; A, C: ESPER_LIR; B, D: ESPER_NN.

surface ΔA_T does not show any clear patterns (Figure S3 in Supporting Information S1). Combining individual transects into groups of regions (see definition of regions in Figure S9 in Supporting Information S1) reduces uncertainties below the calculated trend for only some regions (Figure 5). Trends and uncertainties on a per-region basis are given in Tables S1 and S2 in Supporting Information S1.

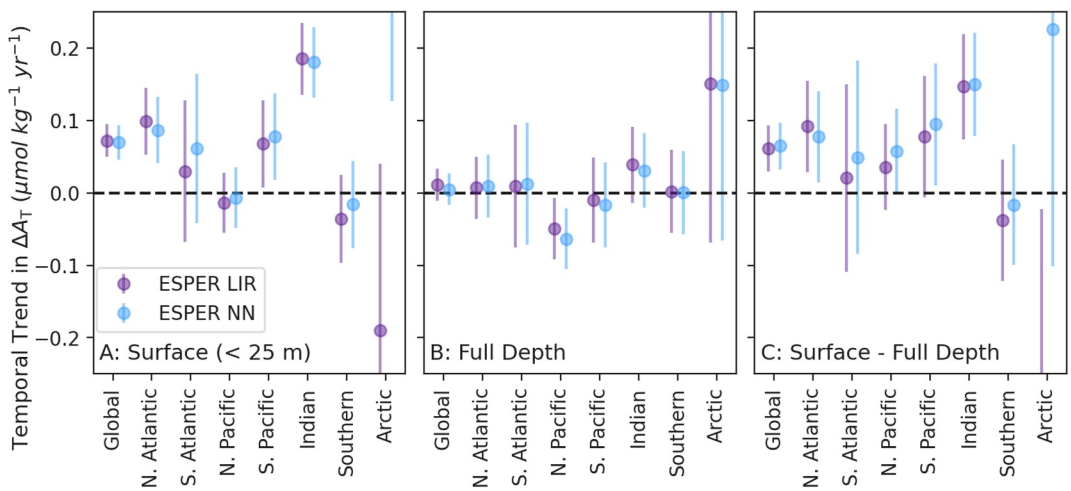

Figure 5. Trend in the difference in measured A_T and ESPER-estimated A_T (ΔA_T) over time for each region. Dark purple points were calculated using ESPER_LIR as counterfactual, and light blue with ESPER_NN. Trends were calculated with robust linear model regression. Subplot A: surface values only (<25 m); subplot B: full depth of measurements available; subplot C: trend in ΔA_T calculated for full depth of measurements subtracted from trend in ΔA_T calculated for surface values only. Error bars represent calculated uncertainties (U) in subplots A and B. In subplot C, the error is calculated by summation in quadrature of the individual uncertainties U of the corresponding surface and full depth ΔA_T trends.

Three regions, the North Atlantic, South Pacific, and Indian Oceans show positive trends in ΔA_T in the surface ocean above the bounds of uncertainty, but only the Indian Ocean shows a non-zero surface ocean trend above the 2σ confidence level (Figure 5a). The North Pacific shows a decreasing trend in ΔA_T that strengthens across the full ocean depth. The Arctic Ocean especially has a high degree of uncertainty, which can be attributed to both the lower frequency of hydrographic measurements in this basin and the higher uncertainty in ESPER predictions, as the Arctic is generally a challenging area for ESPER algorithms (Carter et al., 2021). It should be noted that these trends do not reflect changes in regional A_T caused by shifts in salinity due to the intensification of the water cycle (Fine et al., 2017), but instead represent changes in A_T due to shifts in biological processes, as ESPER algorithms are designed to account for salinity changes (see Section 4.3 for further discussion).

Potential trends in ΔA_T were also examined across different depth ranges (Table S3 in Supporting Information S1). Between 500 and 4,000 m, the vast majority of depth ranges showed no significant trend in ΔA_T, and none showed significance at the 2σ confidence level. At depths below 4,000 m, a negative trend (generally at 1σ confidence) was detected using both ESPER_LIR and ESPER_NN. This may indicate that diminished biotic calcification at the surface or increased near-surface dissolution has resulted in a decreasing export of carbonates to depth, but the low statistical confidence of the trend implies that ESPER or measurement uncertainties are also plausible explanations, given that measurement uncertainties are nearly constant with depth while changes in A_T distributions are generally smaller.

Differences in trends in ΔA_T on a seasonal basis were observed (Tables S4 and S5 in Supporting Information S1). Positive trends in surface ΔA_T at the 2σ confidence level were found in the winter, spring, and autumn months, while no statistically significant trend was detected in summer. No statistically significant seasonal trends at the 2σ confidence level were detected across the full ocean depth. One plausible explanation for the lack of a significant positive trend in surface ΔA_T during summer months could be a decrease in net community production due to shoaling of the mixed layer brought on by enhanced stratification under a changing climate (Fu et al., 2016). Reduced nitrate uptake would result in a lower production of A_T (Brewer et al., 1975; Kanamori & Ikegami, 1982; Wolf-Gladrow et al., 2007), potentially masking decreases in $CaCO_3$ production; however, more research is needed to investigate this hypothesis.

Furthermore, ESPERs are trained on seasonally biased data. 40.1% of the measurements are made in summer, while 18.1%, 13.5%, and 28.3% of the measurements are made in spring, winter, and autumn, respectively. This makes extracting seasonal trends with high confidence challenging. It is also possible that ESPERs have implicitly captured the summertime trend in A_T due to a fairly consistent seasonal distribution of measurements over time (Figure S10 in Supporting Information S1), though this trend would fall within the calculated uncertainties.

4. Discussion

4.1. Regional Trends in ΔA_T

Unlike in the surface ocean, high uncertainties in the underlying processes make it unclear how the deep and intermediate ocean will respond to the CO_2-biotic calcification and export feedback. Subsurface A_T could decrease due to diminished surface export (and thus diminished dissolution) or increase due to higher rates of shelf or water column dissolution. Regardless, models suggest that the deep response should be sluggish in comparison with the surface response (Carter et al., 2016). In contrast, spurious apparent A_T trends from measurement uncertainties or shifts in methods over time could result in trends that span both the deep and surface ocean. Therefore, the difference between the surface trend and the full water column trend might provide a more reliable metric for the impacts of the CO_2-biotic calcification and export feedback.

Indeed, the regional variability, which our Monte Carlo analysis shows to be meaningfully impacted by measurement uncertainties, is diminished when considering this difference metric (Figure 5c). In particular, the larger-than-normal trend in the Indian Ocean and the smaller-than-normal trend in the North Pacific are brought in line with the global trend when this metric is applied. The difference between the surface and full water column trends in ΔA_T is 0.146 ± 0.072 μmol kg^{-1} yr^{-1} in the Indian Ocean and 0.035 ± 0.059 μmol kg^{-1} yr^{-1} in the North Pacific using ESPER_LIR as the counterfactual (Table S1 in Supporting Information S1). Both the Indian (Müller et al., 2023) and the North Pacific (Carter, Sharp, Dickson, et al., 2024) are regions where there have been shifts in A_T measurement and adjustment practices over time, so we contend the surface-to-deep trend difference is likely a

more reliable metric for these regions. Furthermore, this supports our assertion that much of the regional variations we see can be attributed to measurement uncertainties. There may be additional interesting regional patterns to examine during this global signal, but we leave this to future work and maintain that this will remain statistically challenging until more decades of repeated hydrographic A_T measurements are available.

4.2. Sources of Error

Errors in this analysis could arise from long-term trends in predictor variables, biases potentially inherent to ESPER_LIR or ESPER_NN, or biases in GLODAP data. One explanation for the trend in ΔA_T is that the strategy for removing the impacts of natural variations by using ESPERs as counterfactuals relies on predictor information that may also be influenced by separate long-term trends. However, we have used many predictor combinations and shown that variations across regression equations, which variably omit each of the predictors besides S_P, are comparatively small (Figure 2). We have included these variations in our overall trend uncertainty estimate U, and we consider long-term trends in S_P (which is common to all ESPER variants) separately below.

It is also possible that the apparent trend is due to a bias inherent to the structure of ESPER_LIR or ESPER_NN. However, these are independent algorithms trained on nearly identical training data, which indicates that the trend is a product of A_T measurements and not the algorithm used to account for natural variability. It is also possible that the data used to train the algorithms, which includes data from many hydrographic cruises that were never occupied more than once and thus never appear directly within this study, contain a regional or measurement bias. To assess this, the analysis was repeated with a version of ESPER_LIR (ESPER_LIR_GO-SHIP) trained using identical training scripts to those used for ESPER_LIR after limiting the training data to the data used for the ΔA_T calculations in this study (Figure S11 in Supporting Information S1). Statistically equivalent trends in ΔA_T were found with this variant.

Collectively, these observations provide some support for the statement that the results we find are not an artifact of the algorithm used as a counterfactual or its training data. We note that the GLODAPv2 adjustments are made on the basis of reducing apparent mismatches between measurements made by repeated cruises in the deep and interior oceans. It is possible that adjustments made on this basis could reduce or eliminate the deep ocean A_T trend.

4.3. Attribution to CO_2-Biotic Calcification and Export Feedback

To discern if the observed trend in surface ΔA_T can be attributed to the CO_2-biotic calcification and export feedback, other processes affecting the distribution of surface A_T were considered (Fry et al., 2015). These include (a) changes in the rate of riverine discharge of A_T (Cai et al., 2008), (b) increases in A_T input from increased sea ice melt (Rysgaard et al., 2012), (c) dilution of surface A_T by increased land and sea ice melt inputs of freshwater to the surface, (d) changes in the stratification of the ocean and therefore shifts in upwelling patterns of subsurface A_T (Lee et al., 2006), (e) changes in organic matter production and export (Wolf-Gladrow et al., 2007), and (f) trends in A_T distributions due to fluctuations in the ocean's state caused by glacial/interglacial cycles (Yu et al., 2015). For each of these processes, we consider both how this process would change the distribution of alkalinity and the degree to which the empirical ESPER relationships may or may not be expected to counter those changes.

Simple A_T budgets were performed to address processes (a) and (b) and are outlined in Texts S1 in Supporting Information S1 (Cai et al., 2008; Gudmundsson et al., 2021; Stets et al., 2014) and S2 (Dieckmann et al., 2008; Ji et al., 2021; Perovich et al., 2020; Rysgaard et al., 2012; Smith et al., 2020). As a result of increases in the rate of riverine discharge of A_T (process a), we estimate that the rate of surface A_T increase could be up to 0.028 μmol kg^{-1} yr^{-1}, approximately 3 times less than the observed trend in ΔA_T, indicating that this process is not sufficient to explain the observed trend. Increases in the rate of sea ice melt (process b) are similarly less than the observed trend, as we estimate that the rate of surface A_T increase from this process is 0.010 μmol kg^{-1} yr^{-1}, approximately 7 times less than the observed trend.

Process (c), the effect of dilution by freshwater on surface A_T due to increases in melting of both land and sea ice, is addressed with a salinity budget (Text S3; Carter et al., 2014; Cox & Weeks, 1974; Hugonnet et al., 2021; Smith et al., 2020). It is estimated that surface ocean S_P could be decreasing at a rate of up to -0.03 dec^{-1}, which would cause a decrease in surface A_T over time due to dilution with freshwater (Cox & Weeks, 1974; Hugonnet

et al., 2021). ESPERs predict a positive correlation between A_T and S_P, as the average surface ocean coefficient reflecting the sensitivity of A_T to S_P (ΔA_T:ΔS_P) calculated for use in ESPER_LIR is 55 μmol A_T kg^{-1}. This coefficient implies that ESPER-predicted surface A_T could be changing by −0.165 μmol kg^{-1} yr^{-1} (55 μmol A_T kg^{-1} * −0.03 dec^{-1}) due to salinity changes. The global surface ocean A_T:S_P ratio, which can also be considered a slope due to the assumption of a freshwater end-member with zero A_T, is approximately 66.4 μmol A_T kg^{-1} (mean surface ocean A_T and S_P of 2305 μmol kg^{-1} yr^{-1} and 34.71, respectively, are taken from Carter et al., 2014). Therefore, this freshwater would be expected to decrease measured surface ocean A_T by approximately 1.2 (66.4 μmol A_T kg^{-1}/55 μmol A_T kg^{-1}) times as much as it would decrease ESPER-estimated A_T. Thus, this process might be expected to lead to a negative trend in ΔA_T (−0.033 μmol kg^{-1} yr^{-1}).

Intensification of the hydrological cycle is projected to occur under climate change and would influence sea surface salinity distributions (Durack & Wijffels, 2010). Though shifts in evaporation and precipitation patterns locally would not change the global mean value of A_T, this process could affect trends in ΔA_T on a regional scale (Fine et al., 2017). This possibility is explored in Text S4 in Supporting Information S1 (Carter et al., 2014; Durack & Wijffels, 2010). Applying the same methodology used to quantify the effects from potential long-term salinity changes (process c), we find that in the Atlantic, where salinity has increased by 0.078 ± 0.095 from 1950 to 2000 (Durack & Wijffels, 2010), a salinity increase could account for a trend in ΔA_T of +0.022 μmol kg^{-1} yr^{-1}. In the Pacific, which freshened by 0.044 ± 0.064 over the same period (Durack & Wijffels, 2010), there could be a trend in ΔA_T of −0.010 μmol kg^{-1} yr^{-1}. In the Indian Ocean, no significant trend was detected in salinity over this period. Even the most extreme changes in salinity reported by Durack and Wijffels (2010), found only in localized regions, of ±0.2 from 1950 to 2000 would only be expected to produce a localized ΔA_T trend of ±0.05 μmol kg^{-1} yr^{-1}, a number that is still less than the globally averaged trend in ΔA_T.

Changes in stratification could also change the supply of A_T from below the surface mixed layer (process d). However, a related study for nitrate estimated that increases in stratification are leading to a decrease in surface ocean nitrate of −0.18 μmol L^{-1} dec^{-1} (−0.018 μmol kg^{-1} yr^{-1}) as the supply from below declines (Gregg & Rousseaux, 2019). As A_T tends to increase with depth in the ocean (on average), an increase in stratification would be expected to lead to a decrease in surface A_T rather than an increase, and thus this change seems unlikely to explain our observations.

If, however, the decline in surface nitrate is due instead to increased organic matter production and export (process e) with a constant supply of nitrate and A_T and an unchanged carbonate mineral cycle (or a concentration of biological production in a shallower mixed layer), this would be accompanied by an increase in A_T due to charge balance (Brewer et al., 1975; Kanamori & Ikegami, 1982; Wolf-Gladrow et al., 2007). This case represents the extreme other end of the spectrum of the nitrate/A_T relationship. Even when (unrealistically) attributing the surface nitrate decline calculated by Gregg and Rousseaux (2019) entirely to this process, we estimate that the corresponding increase in A_T required to satisfy the charge balance would be 0.024 μmol kg^{-1} yr^{-1}, 3 times less than the observed trend in surface A_T increase (Text S5 in Supporting Information S1; Gregg & Rousseaux, 2019; Wolf-Gladrow et al., 2007).

We also consider the possibility that these processes could bias the trend by decreasing the A_T estimated by ESPERs as surface nitrate is decreasing. ESPERs predict a positive correlation between A_T and nitrate (average surface ocean A_T:nitrate ratio calculated for use as coefficient in ESPER_LIR is 0.110 μmol $μmol^{-1}$), indicating ESPER-predicted surface A_T could have an implicit trend of −0.0020 μmol kg^{-1} yr^{-1} (0.110 μmol A_T [μmol nitrate]$^{-1}$ * −0.018 μmol kg^{-1} yr^{-1}), which is less than 3% of the magnitude of the observed trend (ESPER_LIR, RLM). This sensitivity would only affect predictions from the 50% of ESPER equations that include nitrate as a predictor, so this process would only be expected to change the mean ΔA_T trend by +0.00099 μmol kg^{-1} yr^{-1} even if the supply of surface ocean A_T were somehow unaffected by the decrease in vertical mixing.

This analysis is repeated to determine the possible effects of a bias in ESPER estimates due to a positive trend in sea surface temperature (SST). Garcia-Soto et al. (2021) quantified a global average SST increase of 0.280 ± 0.068°C dec^{-1} from the years 2010–2019. The average surface ocean A_T:T coefficient calculated by ESPERs is −0.338 μmol kg^{-1} A_T $°C^{-1}$, indicating that ESPER-predicted surface A_T could have an implicit trend of −0.0095 μmol kg^{-1} yr^{-1} (−0.338 μmol kg^{-1} A_T $°C^{-1}$ * 0.280°C dec^{-1}). Similar to nitrate, this would only affect 50% of predictions by ESPER equations, therefore biasing the mean ΔA_T trend by +0.0047 μmol kg^{-1} yr^{-1}, which is about 15 times less than the observed trend in ΔA_T.

Due to the effects of glacial/interglacial cycles on the Earth system (process f), it cannot be assumed that A_T distributions in the ocean were in a steady state prior to the industrial era. However, literature suggests that A_T in the surface ocean was likely to decrease slightly during the pre-industrial Holocene (Brovkin et al., 2019; Elsig et al., 2009; Yu et al., 2015). As implicit biases in the salinity and nitrate predictor variables, which represent abiotic and biotic processes, have already been addressed, it is unlikely that a non-steady state ocean is causing the observed trend in ΔA_T and instead it seems likely that anthropogenic effects are at the root of this change.

4.4. Possible Biological and Chemical Mechanisms

There are four mechanisms related to biotic calcification that could lead to the observed increase in surface ocean alkalinity. First, calcifying organisms could be preferentially decreasing their rates of calcification over time. Alternatively, the number of calcifying organisms in the ocean could be decreasing. Third, it is possible that sedimentary carbonates are being preferentially redissolved instead of buried due to an acidifying ocean. Finally, the rate of dissolution of carbonates in shallow waters could be increasing, and thus the export of alkalinity from the surface ocean could be decreasing or the exported alkalinity could be increasingly redissolved at shallow depth and returned to the surface through mixing processes. We did not find sufficient observational evidence to distinguish between these mechanisms.

Some of these four mechanisms might be expected to result in different signals in alkalinity distributions, as explored to some extent by Liang et al. (2023). These authors assess how well model simulations of various carbonate mineral dissolution mechanisms reconstruct the observed alkalinity distribution. They note that several dissolution processes result in similar preformed and excess alkalinity distributions, and that the best match is found for constant-dissolution with depth or dissolution that is partially mediated by respiration in the upper ocean. Our approach is focused on small changes in the ocean alkalinity distribution over several decades rather than the shape of the global alkalinity distribution, which results from processes acting over the thousand year timescales of ocean overturning. For this reason, our approach is even less well-suited to reveal the exact processes behind the observed trend. We are therefore unable to distinguish between these mechanisms on the basis of our findings.

A review of laboratory studies has found mixed responses of all calcifying species to ocean acidification (Leung et al., 2022), though for calcifying plankton, a decrease in calcification rates is often observed under ocean acidification scenarios (Bednaršek et al., 2019; Kuroyanagi et al., 2021; Meyer & Riebesell, 2015). Furthermore, the magnitude of the observed trend in surface ocean ΔA_T is relatively small compared to uncertainty in satellite-based measurements of particulate inorganic carbon (PIC), which estimate the average amount of $CaCO_3$ produced annually by coccolithophores to be 1.42 ± 1.69 PgC (Hopkins & Balch, 2018). Nevertheless, we believe we have shown that the carbonate system is not in steady state in the anthropocene and that our findings are consistent with the CO_2-biotic calcification and export/burial feedback hypothesis.

4.5. Applications to Marine Carbon Dioxide Removal

New technologies, referred to as marine carbon dioxide removal (mCDR), have been proposed to harness the ocean's capacity as a carbon sink to store atmospheric CO_2 (National Academies of Sciences et al., 2022). One technique, ocean alkalinity enhancement (OAE), involves elevating levels of A_T in the surface ocean such that atmospheric CO_2 is drawn down as the surface ocean and atmosphere re-equilibrates via air-sea gas exchange (Kheshgi, 1995; Renforth & Henderson, 2017). By some measures, OAE is a "reverse experiment" for ocean acidification. In an OAE scenario, instead of an accumulation of surface A_T, the CO_2-biotic calcification feedback would cause a reduction in surface A_T as some of the additional A_T from OAE is diverted to biotic calcification. This would result in a loss of efficiency for an OAE deployment because precipitation of carbonate minerals in seawater drives CO_2 from the ocean to the atmosphere in a ratio of about 0.6–0.7 mol CO_2 per mole precipitated CO_3^{2-} (Frankignoulle et al., 1994), which would need to be accounted for to accurately determine the amount of CO_2 removed from the atmosphere. This study provides an observational constraint on what the magnitude of this inefficiency could be in an OAE operation, indicating that while the CO_2-biotic calcification feedback will not likely be a large loss term, it should be counted in the overall budget. Furthermore, the trend in A_T found in this study implies that long-term evaluation of OAE may need to account for non-steady state trends in the "natural" alkalinity cycle.

However, increased rates of calcification due to an influx of A_T could cause other changes in an OAE scenario. Higher levels of $CaCO_3$ could potentially act to increase the amount of ballast material for particulate organic carbon, which could increase the efficiency or remineralization length scale of biological carbon export, which is known as the "more ballast feedback mechanism" (Bach et al., 2019). This could potentially oppose the reduction in available alkalinity due to the CO_2-biotic calcification feedback to some degree. Further research must be done to clarify the relative strength of these processes in order to quantify their effects on carbon export during an OAE deployment.

5. Conclusions

Algorithms designed to predict seawater properties, including total alkalinity (A_T), are used as a counterfactual to extract a trend in surface A_T measurements performed on repeat hydrographic cruises. This >30 years trend can likely be attributed to the hypothesized CO_2-biotic calcification feedback, in which increasing oceanic CO_2 uptake, worsening ocean acidification, and decreasing rates of biotic calcification and export cause accumulation in surface A_T. Over the past 30 years, approximately 20 Tmol of additional A_T has accumulated in the surface ocean due to this buildup, equivalent to over half the annual input of A_T via riverine sources (Cai et al., 2008). Assuming complete equilibration, this would have increased the ocean anthropogenic carbon burden by an estimated 0.2%, or 0.20 PgC (Text S6 in Supporting Information S1, Carter et al., 2014; Humphreys et al., 2022; Lan & Keeling, n.d.). This does not account for the potential impacts of reduced calcification on the biological carbon pump, such as a decreased flux of organic carbon to the deep sea due to lower availability of $CaCO_3$ ballast materials (Riebesell et al., 2009).

It is well understood that marine anthropogenic CO_2 accumulation has influenced ocean carbonate chemistry and decreased the ocean's capacity to store additional atmospheric CO_2. Our findings here point to a global slowdown in biotic calcification and export and a resulting buildup in surface A_T, which increases the surface ocean's ability to uptake CO_2. In summary, we contend that anthropogenic CO_2 emissions are quantifiably changing the processes by which the marine carbon cycle regulates Earth's climate on a planetary scale, likely by disrupting patterns in the life cycles of calcifying organisms. Ocean acidification is now both a symptom and a cause of measurable anthropogenic perturbations to the global carbon cycle.

Though signatures of the CO_2-biotic calcification feedback can be detected on a global scale, we do not have enough repeat hydrographic measurements to assess how the feedback operates on a regional basis or along individual cruise transects. Understanding this phenomenon on a local scale would be necessary to project changes in key ecosystems under climate change and to accurately model the carbon uptake of mCDR deployments. A larger scale of measurements, especially in rapidly changing and relatively under-sampled regions such as the Arctic, would enable us to place further constraints on the effect of this feedback within the marine carbon cycle.

Data Availability Statement

The GLODAPv2.2023 data used in the study are available at the National Oceanic and Atmospheric Administration (NOAA)'s National Centers for Environmental Information (NCEI) Ocean Carbon and Acidification Data System (OCADS) via https://www.ncei.noaa.gov/data/oceans/ncei/ocads/data/0283442/.

* Lauvset et al. (2022, 2023) and Olsen et al. (2019, 2020).

The Empirical Seawater Property Estimation Routines (ESPERs) used for the prediction of alkalinity co-located with GLODAP measurements are preserved at https://github.com/BRCScienceProducts/ESPER and developed by B. R. Carter.

* Carter et al. (2021).

The PyCO2SYS software package used for calculations in Text S6 in Supporting Information S1 is available at https://zenodo.org/records/14506565.

* Humphreys et al. (2022).

Atmospheric carbon dioxide concentrations used for calculations in Text S6 in Supporting Information S1 are available at https://gml.noaa.gov/ccgg/trends/data.html.

* Lan and Keeling (n.d.).

Acknowledgments
RCB and BRC thank the National Oceanographic Partnership Program (NOPP) for support through the Inflation Reduction Act under the National Oceanic and Atmospheric Administration's Ocean Acidification Program award NA23OAR0170515 to University of Washington. Analyses used to explore uncertainties in ESPER estimates and measurements were enabled by support from the Global Ocean Monitoring and Observing program of NOAA through funding the Carbon Data Management and Synthesis Program (Fund Ref. 100007298, program officer: Kathy Tedesco). AJF was supported by NOAA's Pacific Marine Environmental Laboratory (PMEL). BT was supported by CSIRO Environment and the Australian Antarctic Program Partnership. RJW was supported by the National Science Foundation Division of Ocean Sciences (OCE-2148468). KAS was supported by the Atlantic Zone Offshore Monitoring Programme (AZOMP) and the Aquatic Climate Change Adaptation Services Program (ACCASP) of Fisheries and Oceans, Canada. MI was supported by the Environmental Research and Technology Development Fund (JPMEERF24S12200) of the Environmental Restoration and Conservation Agency provided by the Ministry of the Environment of Japan. FFP was supported by the BOCATS2 (PID2019-104279GB-C21) project funded by MCIN/AEI/10.13039/501100011033 and by the European Union under grant agreement no. 101094690 (EuroGO-SHIP). PMEL and CICOES contributions are numbers 5657 and 2024-1405, respectively. The authors would also like to extend their gratitude to the many people who have played a role in the collection of alkalinity data preserved in GLODAP, including Frank Millero, Andrew Dickson, Kazuhiro Nemoto, Christopher Sabine, Douglas Wallace, Hitomi Kamiya, Christopher Winn, Robert Key, E. Peter Jones, Aida Fernández Ríos, and every other scientist, technician, and crew member who contributed countless hours of effort to this data set.

References

Andersen, R. (2007). *Modern methods for robust regression*. Sage Publications, Inc. https://doi.org/10.4135/9781412985109

Bach, L. T., Gill, S. J., Rickaby, R. E. M., Gore, S., & Renforth, P. (2019). CO_2 removal with enhanced weathering and ocean alkalinity enhancement: Potential risks and co-benefits for marine pelagic ecosystems. *Frontiers in Climate*, *1*. https://doi.org/10.3389/fclim.2019.00007

Bednaršek, N., Feely, R. A., Howes, E. L., Hunt, B. P. V., Kessouri, F., León, P., et al. (2019). Systematic review and meta-analysis toward synthesis of thresholds of ocean acidification impacts on calcifying pteropods and interactions with warming. *Frontiers in Marine Science*, *6*. https://doi.org/10.3389/fmars.2019.00227

Berelson, W. M., Balch, W. M., Najjar, R., Feely, R. A., Sabine, C., & Lee, K. (2007). Relating estimates of $CaCO_3$ production, export, and dissolution in the water column to measurements of $CaCO_3$ rain into sediment traps and dissolution on the sea floor: A revised global carbonate budget. *Global Biogeochemical Cycles*, *21*(1). https://doi.org/10.1029/2006GB002803

Bockmon, E. E., & Dickson, A. G. (2015). An inter-laboratory comparison assessing the quality of seawater carbon dioxide measurements. *Marine Chemistry*, *171*, 36–43. https://doi.org/10.1016/j.marchem.2015.02.002

Boudreau, B. P., Middelburg, J. J., & Luo, Y. (2018). The role of calcification in carbonate compensation. *Nature Geoscience*, *11*(12), 894–900. https://doi.org/10.1038/s41561-018-0259-5

Brewer, P. G., Wong, G. T. F., Bacon, M. P., & Spencer, D. W. (1975). An oceanic calcium problem? *Earth and Planetary Science Letters*, *26*(1), 81–87. https://doi.org/10.1016/0012-821X(75)90179-X

Brovkin, V., Lorenz, S., Raddatz, T., Ilyina, T., Stemmler, I., Toohey, M., & Claussen, M. (2019). What was the source of the atmospheric CO_2 increase during the Holocene? *Biogeosciences*, *16*(13), 2543–2555. https://doi.org/10.5194/bg-16-2543-2019

Cai, W.-J., Guo, X., Chen, C.-T. A., Dai, M., Zhang, L., Zhai, W., et al. (2008). A comparative overview of weathering intensity and HCO_3^- flux in the world's major rivers with emphasis on the Changjiang, Huanghe, Zhujiang (Pearl) and Mississippi Rivers. *Continental Shelf Research*, *28*(12), 1538–1549. https://doi.org/10.1016/j.csr.2007.10.014

Carter, B. R., Bittig, H. C., Fassbender, A. J., Sharp, J. D., Takeshita, Y., Xu, Y.-Y., et al. (2021). New and updated global empirical seawater property estimation routines. *Limnology and Oceanography: Methods*, *19*(12), 785–809. https://doi.org/10.1002/lom3.10461

Carter, B. R., Feely, R. A., Wanninkhof, R., Kouketsu, S., Sonnerup, R. E., Pardo, P. C., et al. (2019). Pacific anthropogenic carbon between 1991 and 2017. *Global Biogeochemical Cycles*, *33*(5), 597–617. https://doi.org/10.1029/2018GB006154

Carter, B. R., Feely, R. A., Williams, N. L., Dickson, A. G., Fong, M. B., & Takeshita, Y. (2018). Updated methods for global locally interpolated estimation of alkalinity, pH, and nitrate. *Limnology and Oceanography: Methods*, *16*(2), 119–131. https://doi.org/10.1002/lom3.10232

Carter, B. R., Frölicher, T. L., Dunne, J. P., Rodgers, K. B., Slater, R. D., & Sarmiento, J. L. (2016). When can ocean acidification impacts be detected from decadal alkalinity measurements? *Global Biogeochemical Cycles*, *30*(4), 595–612. https://doi.org/10.1002/2015GB005308

Carter, B. R., Sharp, J. D., Dickson, A. G., Álvarez, M., Fong, M. B., García-Ibáñez, M. I., et al. (2024). Uncertainty sources for measurable ocean carbonate chemistry variables. *Limnology & Oceanography*, *69*(1), 1–21. https://doi.org/10.1002/lno.12477

Carter, B. R., Sharp, J. D., García-Ibáñez, M. I., Woosley, R. J., Fong, M. B., Álvarez, M., et al. (2024). Random and systematic uncertainty in ship-based seawater carbonate chemistry observations. *Limnology & Oceanography*, *69*(10), 2473–2488. https://doi.org/10.1002/lno.12674

Carter, B. R., Toggweiler, J. R., Key, R. M., & Sarmiento, J. L. (2014). Processes determining the marine alkalinity and calcium carbonate saturation state distributions. *Biogeosciences*, *11*(24), 7349–7362. https://doi.org/10.5194/bg-11-7349-2014

Cox, G. F. N., & Weeks, W. F. (1974). Salinity variations in sea ice. *Journal of Glaciology*, *13*(67), 109–120. https://doi.org/10.3189/S0022143000023418

Dickson, A. G. (1981). An exact definition of total alkalinity and a procedure for the estimation of alkalinity and total inorganic carbon from titration data. *Deep-Sea Research, Part A: Oceanographic Research Papers*, *28*(6), 609–623. https://doi.org/10.1016/0198-0149(81)90121-7

Dickson, A. G., Afghan, J. D., & Anderson, G. C. (2003). Reference materials for oceanic CO_2 analysis: A method for the certification of total alkalinity. *Marine Chemistry*, *80*(2), 185–197. https://doi.org/10.1016/S0304-4203(02)00133-0

Dickson, A. G., Sabine, C. L., & Christian, J. R. (2007). In *Guide to best practices for ocean CO_2 measurements* (Vol. 3). PICES Special Publication. Retrieved from https://www.ncei.noaa.gov/access/ocean-carbon-acidification-data-system/oceans/Handbook_2007.html

Dieckmann, G. S., Nehrke, G., Papadimitriou, S., Göttlicher, J., Steininger, R., Kennedy, H., et al. (2008). Calcium carbonate as ikaite crystals in Antarctic sea ice. *Geophysical Research Letters*, *35*(8). https://doi.org/10.1029/2008GL033540

Doney, S. C., Busch, D. S., Cooley, S. R., & Kroeker, K. J. (2020). The impacts of ocean acidification on marine ecosystems and reliant human communities. *Annual Review of Environment and Resources*, *45*(1), 83–112. https://doi.org/10.1146/annurev-environ-012320-083019

Doney, S. C., Fabry, V. J., Feely, R. A., & Kleypas, J. A. (2009). Ocean acidification: The other CO_2 problem. *Annual Review of Marine Science*, *1*, 169–192. https://doi.org/10.1146/annurev.marine.010908.163834

Durack, P. J., & Wijffels, S. E. (2010). Fifty-year trends in global ocean salinities and their relationship to broad-scale warming. *Journal of Climate*, *23*(16), 4342–4362. https://doi.org/10.1175/2010JCLI3377.1

Elsig, J., Schmitt, J., Leuenberger, D., Schneider, R., Eyer, M., Leuenberger, M., et al. (2009). Stable isotope constraints on Holocene carbon cycle changes from an Antarctic ice core. *Nature*, *461*(7263), 507–510. https://doi.org/10.1038/nature08393

Fine, R. A., Willey, D. A., & Millero, F. J. (2017). Global variability and changes in ocean total alkalinity from Aquarius satellite data. *Geophysical Research Letters*, *44*(1), 261–267. https://doi.org/10.1002/2016GL071712

Frankignoulle, M., Canon, C., & Gattuso, J.-P. (1994). Marine calcification as a source of carbon dioxide: Positive feedback of increasing atmospheric CO_2. *Limnology & Oceanography*, *39*(2), 458–462. https://doi.org/10.4319/lo.1994.39.2.0458

Friedlingstein, P., O'Sullivan, M., Jones, M. W., Andrew, R. M., Bakker, D. C. E., Hauck, J., et al. (2023). Global carbon budget 2023. *Earth System Science Data*, *15*(12), 5301–5369. https://doi.org/10.5194/essd-15-5301-2023

Fry, C. H., Tyrrell, T., Hain, M. P., Bates, N. R., & Achterberg, E. P. (2015). Analysis of global surface ocean alkalinity to determine controlling processes. *Marine Chemistry*, *174*, 46–57. https://doi.org/10.1016/j.marchem.2015.05.003

Fu, W., Randerson, J. T., & Moore, J. K. (2016). Climate change impacts on net primary production (NPP) and export production (EP) regulated by increasing stratification and phytoplankton community structure in the CMIP5 models. *Biogeosciences*, *13*(18), 5151–5170. https://doi.org/10.5194/bg-13-5151-2016

Garcia-Soto, C., Cheng, L., Caesar, L., Schmidtko, S., Jewett, E. B., Cheripka, A., et al. (2021). An overview of ocean climate change indicators: Sea surface temperature, ocean heat content, ocean pH, dissolved oxygen concentration, Arctic sea ice extent, thickness and volume, sea level and strength of the AMOC (Atlantic meridional overturning circulation). *Frontiers in Marine Science*, *8*. https://doi.org/10.3389/fmars.2021.642372

Gattuso, J.-P., Magnan, A., Billé, R., Cheung, W. W. L., Howes, E. L., Joos, F., et al. (2015). Contrasting futures for ocean and society from different anthropogenic CO_2 emissions scenarios. *Science*, *349*(6243), aac4722. https://doi.org/10.1126/science.aac4722

Gregg, W. W., & Rousseaux, C. S. (2019). Global ocean primary production trends in the modern ocean color satellite record (1998–2015). *Environmental Research Letters*, *14*(12), 124011. https://doi.org/10.1088/1748-9326/ab4667

Gruber, N., Bakker, D. C. E., DeVries, T., Gregor, L., Hauck, J., Landschützer, P., et al. (2023). Trends and variability in the ocean carbon sink. *Nature Reviews Earth and Environment*, *4*(2), 119–134. https://doi.org/10.1038/s43017-022-00381-x

Gudmundsson, L., Boulange, J., Do, H. X., Gosling, S. N., Grillakis, M. G., Koutroulis, A. G., et al. (2021). Globally observed trends in mean and extreme river flow attributed to climate change. *Science*, *371*(6534), 1159–1162. https://doi.org/10.1126/science.aba3996

Heinze, C. (2004). Simulating oceanic $CaCO_3$ export production in the greenhouse. *Geophysical Research Letters*, *31*(16). https://doi.org/10.1029/2004GL020613

Holte, J., Talley, L. D., Gilson, J., & Roemmich, D. (2017). An Argo mixed layer climatology and database. *Geophysical Research Letters*, *44*(11), 5618–5626. https://doi.org/10.1002/2017GL073426

Hopkins, J., & Balch, W. M. (2018). A new approach to estimating coccolithophore calcification rates from space. *Journal of Geophysical Research: Biogeosciences*, *123*(5), 1447–1459. https://doi.org/10.1002/2017JG004235

Hugonnet, R., McNabb, R., Berthier, E., Menounos, B., Nuth, C., Girod, L., et al. (2021). Accelerated global glacier mass loss in the early twenty-first century. *Nature*, *592*(7856), 726–731. https://doi.org/10.1038/s41586-021-03436-z

Humphreys, M. P., Lewis, E. R., Sharp, J. D., & Pierrot, D. (2022). PyCO2SYS v1.8: Marine carbonate system calculations in Python. *Geoscientific Model Development*, *15*(1), 15–43. https://doi.org/10.5194/gmd-15-15-2022

Ilyina, T., Zeebe, R. E., Maier-Reimer, E., & Heinze, C. (2009). Early detection of ocean acidification effects on marine calcification. *Global Biogeochemical Cycles*, *23*(1). https://doi.org/10.1029/2008GB003278

Ji, Q., Li, B., Pang, X., Zhao, X., & Lei, R. (2021). Arctic sea ice density observation and its impact on sea ice thickness retrieval from CryoSat–2. *Cold Regions Science and Technology*, *181*, 103177. https://doi.org/10.1016/j.coldregions.2020.103177

Jiang, L.-Q., Dunne, J., Carter, B. R., Tjiputra, J. F., Terhaar, J., Sharp, J. D., et al. (2023). Global surface ocean acidification indicators from 1750 to 2100. *Journal of Advances in Modeling Earth Systems*, *15*(3), e2022MS003563. https://doi.org/10.1029/2022MS003563

Kanamori, S., & Ikegami, H. (1982). Calcium-alkalinity relationship in the North Pacific. *Journal of the Oceanographical Society of Japan*, *38*(2), 57–62. https://doi.org/10.1007/BF02110291

Kheshgi, H. S. (1995). Sequestering atmospheric carbon dioxide by increasing ocean alkalinity. *Energy*, *20*(9), 915–922. https://doi.org/10.1016/0360-5442(95)00035-F

Kuroyanagi, A., Irie, T., Kinoshita, S., Kawahata, H., Suzuki, A., Nishi, H., et al. (2021). Decrease in volume and density of foraminiferal shells with progressing ocean acidification. *Scientific Reports*, *11*(1), 19988. https://doi.org/10.1038/s41598-021-99427-1

Lan, X., & Keeling, C. D. (n.d.). NOAA global monitoring laboratory and scripps institute of oceanography Mauna Loa observatory CO_2 records [Dataset]. *National Oceanic and Atmospheric Administration Global Monitoring Laboratory*. Retrieved from https://gml.noaa.gov/ccgg/trends/data.html

Lauvset, S. K., Lange, N., Tanhua, T., Bittig, H. C., Olsen, A., Kozyr, A., et al. (2022). GLODAPv2.2022: The latest version of the global interior ocean biogeochemical data product. *Earth System Science Data*, *14*(12), 5543–5572. https://doi.org/10.5194/essd-14-5543-2022

Lauvset, S. K., Lange, N., Tanhua, T., Bittig, H. C., Olsen, A., Kozyr, A., et al. (2023). Global ocean data analysis project version 2.2023 (GLODAPv2.2023) [Dataset]. *NCEI*. https://doi.org/10.13039/100000001

Lee, K., Tong, L. T., Millero, F. J., Sabine, C. L., Dickson, A. G., Goyet, C., et al. (2006). Global relationships of total alkalinity with salinity and temperature in surface waters of the world's oceans. *Geophysical Research Letters*, *33*(19). https://doi.org/10.1029/2006GL027207

Leung, J. Y. S., Zhang, S., & Connell, S. D. (2022). Is Ocean acidification really a threat to marine calcifiers? A systematic review and meta-analysis of 980+ studies spanning two decades. *Small*, *18*(35), 2107407. https://doi.org/10.1002/smll.202107407

Liang, H., Lunstrum, A. M., Dong, S., Berelson, W. M., & John, S. G. (2023). Constraining $CaCO_3$ export and dissolution with an ocean alkalinity inverse model. *Global Biogeochemical Cycles*, *37*(2), e2022GB007535. https://doi.org/10.1029/2022GB007535

Ma, D., Gregor, L., & Gruber, N. (2023). Four decades of trends and drivers of global surface Ocean Acidification. *Global Biogeochemical Cycles*, *37*(7), e2023GB007765. https://doi.org/10.1029/2023GB007765

Meyer, J., & Riebesell, U. (2015). Reviews and syntheses: Responses of coccolithophores to ocean acidification: A meta-analysis. *Biogeosciences*, *12*(6), 1671–1682. https://doi.org/10.5194/bg-12-1671-2015

Milliman, J. D. (1993). Production and accumulation of calcium carbonate in the ocean: Budget of a nonsteady state. *Global Biogeochemical Cycles*, *7*(4), 927–957. https://doi.org/10.1029/93GB02524

Milliman, J. D., Troy, P. J., Balch, W. M., Adams, A. K., Li, Y.-H., & Mackenzie, F. T. (1999). Biologically mediated dissolution of calcium carbonate above the chemical lysocline? *Deep Sea Research Part I: Oceanographic Research Papers*, *46*(10), 1653–1669. https://doi.org/10.1016/S0967-0637(99)00034-5

Müller, J. D., Gruber, N., Carter, B., Feely, R., Ishii, M., Lange, N., et al. (2023). Decadal trends in the oceanic storage of anthropogenic carbon from 1994 to 2014. *AGU Advances*, *4*(4), e2023AV000875. https://doi.org/10.1029/2023AV000875

National Academies of Sciences, Engineering, and Medicine. (2022). *A research strategy for ocean-based carbon dioxide removal and sequestration*. The National Academies Press.

Olsen, A., Lange, N., Key, R. M., Tanhua, T., Álvarez, M., Becker, S., et al. (2019). GLODAPv2.2019—An update of GLODAPv2. *Earth System Science Data*, *11*(3), 1437–1461. https://doi.org/10.5194/essd-11-1437-2019

Olsen, A., Lange, N., Key, R. M., Tanhua, T., Bittig, H. C., Kozyr, A., et al. (2020). An updated version of the global interior ocean biogeochemical data product, GLODAPv2.2020. *Earth System Science Data*, *12*(4), 3653–3678. https://doi.org/10.5194/essd-12-3653-2020

Perovich, D., Meier, W., Tschudi, M., Hendricks, S., Petty, A. A., Divine, D., et al. (2020). Sea ice. In *NOAA Arctic report card: Update for 2020*. https://doi.org/10.25923/n170-9h57

Plancherel, Y., Rodgers, K. B., Key, R. M., Jacobson, A. R., & Sarmiento, J. L. (2013). Role of regression model selection and station distribution on the estimation of oceanic anthropogenic carbon change by eMLR. *Biogeosciences*, *10*(7), 4801–4831. https://doi.org/10.5194/bg-10-4801-2013

Renforth, P., & Henderson, G. (2017). Assessing ocean alkalinity for carbon sequestration. *Reviews of Geophysics*, *55*(3), 636–674. https://doi.org/10.1002/2016RG000533

Ridgwell, A., Zondervan, I., Hargreaves, J. C., Bijma, J., & Lenton, T. M. (2007). Assessing the potential long-term increase of oceanic fossil fuel CO_2 uptake due to CO_2-calcification feedback. *Biogeosciences*, *4*(4), 481–492. https://doi.org/10.5194/bg-4-481-2007

Riebesell, U., Körtzinger, A., & Oschlies, A. (2009). Sensitivities of marine carbon fluxes to ocean change. *Proceedings of the National Academy of Sciences of the United States of America*, *106*(49), 20602–20609. https://doi.org/10.1073/pnas.0813291106

Rysgaard, S., Glud, R. N., Lennert, K., Cooper, M., Halden, N., Leakey, R. J. G., et al. (2012). Ikaite crystals in melting sea ice—Implications for pCO_2 and pH levels in Arctic surface waters. *The Cryosphere*, *6*(4), 901–908. https://doi.org/10.5194/tc-6-901-2012

Schlunegger, S., Rodgers, K. B., Sarmiento, J. L., Frölicher, T. L., Dunne, J. P., Ishii, M., & Slater, R. (2019). Emergence of anthropogenic signals in the ocean carbon cycle. *Nature Climate Change*, *9*(9), 719–725. https://doi.org/10.1038/s41558-019-0553-2

Sharp, J. D., & Byrne, R. H. (2020). Interpreting measurements of total alkalinity in marine and estuarine waters in the presence of proton-binding organic matter. *Deep Sea Research Part I: Oceanographic Research Papers*, *165*, 103338. https://doi.org/10.1016/j.dsr.2020.103338

Smith, B., Fricker, H. A., Gardner, A. S., Medley, B., Nilsson, J., Paolo, F. S., et al. (2020). Pervasive ice sheet mass loss reflects competing ocean and atmosphere processes. *Science*, *368*(6496), 1239–1242. https://doi.org/10.1126/science.aaz5845

Stets, E. G., Kelly, V. J., & Crawford, C. G. (2014). Long-term trends in alkalinity in large rivers of the conterminous US in relation to acidification, agriculture, and hydrologic modification. *Science of the Total Environment*, *488–489*, 280–289. https://doi.org/10.1016/j.scitotenv.2014.04.054

Subhas, A. V., Dong, S., Naviaux, J. D., Rollins, N. E., Ziveri, P., Gray, W., et al. (2022). Shallow calcium carbonate cycling in the North Pacific Ocean. *Global Biogeochemical Cycles*, *36*(5), e2022GB007388. https://doi.org/10.1029/2022GB007388

Wolf-Gladrow, D. A., Zeebe, R. E., Klaas, C., Körtzinger, A., & Dickson, A. G. (2007). Total alkalinity: The explicit conservative expression and its application to biogeochemical processes. *Marine Chemistry*, *106*(1), 287–300. https://doi.org/10.1016/j.marchem.2007.01.006

Yu, J., Anderson, R. F., & Rohling, E. J. (2015). Deep Ocean carbonate chemistry and glacial-interglacial atmospheric CO_2 changes. *Oceanography*, *27*(1), 16–25. https://doi.org/10.5670/oceanog.2014.04

Zhang, H., & Cao, L. (2016). Simulated effect of calcification feedback on atmospheric CO_2 and ocean acidification. *Scientific Reports*, *6*(1), 20284. Article 1. https://doi.org/10.1038/srep20284

Zondervan, I., Zeebe, R. E., Rost, B., & Riebesell, U. (2001). Decreasing marine biogenic calcification: A negative feedback on rising atmospheric pCO_2. *Global Biogeochemical Cycles*, *15*(2), 507–516. https://doi.org/10.1029/2000GB001321

Erratum

The originally published version of this article contained typographical errors. The process identifiers have been changed in Section 4.3. In addition, the supporting information has been updated. This may be considered the authoritative version of record.